Analytic spectra of CMB anisotropies and polarization generated by relic gravitational waves with modification due to neutrino free-streaming

T. Y. Xia and Y. Zhang*

Astrophysics Center, University of Science and Technology of China, Hefei, Anhui, China

(Received 12 October 2008; published 11 December 2008)

We present an analytical calculation of the spectra of CMB anisotropies and polarizations generated by relic gravitational waves (RGWs). As a substantial extension to the previous studies, three new ingredients are included in this work. First, the analytic C_l^{TT} and C_l^{TE} are given; especially the latter can be useful to extract signal of RGWs from the observed data in the zero-multipole method. Second, a fitting formula of the decaying factor on small scales is given, coming from the visibility function around the photon decoupling. Third, the impacts by the neutrino free-streaming (NFS) is examined, a process that occurred in the early universe and leaves observable imprints on CMB via RGWs. It is found that the analytic C_l^{TT} and C_l^{TE} have profiles agreeing with the numeric ones, except that C_l^{TT} in a range $l \leq 10$ and the first trough of C_l^{TE} around $l \sim 75$ have some deviations. With the new damping factor, the analytic C_l^{EE} and C_l^{BB} match with the numeric ones with the maximum errors only $\sim 3\%$ up to the first three peaks for $l \leq 600$, improving the previous studies substantially. The correspondence of the positions of peaks of C_l^{XX} and those of RGWs are also demonstrated explicitly. We also find that NFS reduces the amplitudes of C_l^{XX} by $(20\% \sim 35\%)$ for $l \simeq (100 \sim 600)$ and shifts slightly their peaks to smaller angles. Detailed analyses show that the zero multipoles l_0, where C_l^{TE} crosses 0, are shifted to larger values by NFS. This shifting effect is as important as those caused by different inflation models and different baryon fractions.

DOI: 10.1103/PhysRevD.78.123005 PACS numbers: 98.70.Vc, 04.30.Nk, 95.85.Ry, 98.80.−k

I. INTRODUCTION

The observations on cosmic microwave background (CMB) [1–8] are in good agreement with a spatially flat universe with nearly scale-invariant spectrum of primordial adiabatic perturbations predicted by the inflation model. Generally, two kinds of perturbations of the spacetime metric are of interest: density perturbations, i.e. scalar type [9,10] and relic gravitational wave (RGW), i.e. tensorial type [11–18], respectively. Both perturbations will influence the CMB anisotropies and polarizations through the Boltzmann equation for photons. Although the contribution from density perturbation is dominant, RGWs may have important contributions [7]. In particular, as a special feature, RGWs can give rise to a magnetic type of CMB polarizations, and this could provide a distinguished way to directly detect RGWs of very long wavelength comparable to the Hubble radius $\sim 1/H_0$. In comparison, the usual laser interferometers, such as LIGO, probe the intermediate frequency range $\nu = 50$–1000 Hz [19], the waveguide detectors probe the high frequency range $\nu = 10^5$–10^7 Hz [20,21], and the Gaussian laser beam detectors probe in very high frequencies $\nu \sim 10^{10}$ Hz [22,23].

The spectra of CMB anisotropies and polarizations generated by RGWs have long been computed [24–29]. In particular, by approximate treatments of the photon decoupling, Refs. [30,31] have derived the analytic expressions of the polarization spectra, C_l^{EE} and C_l^{BB}, which show explicitly the influences of RGWs, the inflation, the decoupling process, the baryons, and the dark energy, etc. But, compared with the numeric computations, these analytic C_l^{EE} and C_l^{BB} have large errors and are valid only in a limited region of $l \leq 300$. This is largely due to the fact that the damping factor $D(k)$ coming from the visibility function during the decoupling is not accurate enough on small scales. Thus, improvements of accuracy and extensions to a broader range are certainly desired. We will present a fitting formula of $D(k)$, which substantially improves both the accuracy and the region of validity over the previous studies.

Moreover, in the previous analytic calculations [30,31], the cross spectrum C_l^{TE} was not given, neither was the temperature spectrum C_l^{TT}. Theoretically, the magnetic type of polarization C_l^{BB} can only be generated by RGWs. But the current observed data of C_l^{BB} is not yet sufficient to confirm the existence of RGWs [4–8]. On the other hand, the cross spectrum C_l^{TE} is about two orders higher than C_l^{BB} and also contains the contribution from RGWs beside the density perturbations. More importantly, WMAP5 has detected C_l^{TE} [7]. This gives rise to the possibility of extracting RGWs, since the contributions from the scalar and tensorial perturbations behave differently. In particular, RGWs can change the value of the multipole l_0, where C_l^{TE} first crosses 0. Thereby, one can, in principle, tell whether there is a contribution from RGWs and give constraints on the scalar/tensor ratio and other cosmological parameters. This so-called zero-multipole method relies on the detailed analysis of C_l^{TE} [32,33]. Since C_l^{TE} depends on several cosmological parameters, analytic results are always helpful in exhibiting their prop-

*yzh@ustc.edu.cn

 © 2008 The American Physical Society

erties. In this paper we give the analytic C_l^{TE}, as well as C_l^{TT}, due to RGWs.

As a source to CMB, the RGWs depend on the inflation and on the dark energy [34]. Besides, they also depend on physical processes in the radiation-dominated universe, such as neutrino free-streaming (NFS) [35–38], the QCD transition, and the $e^{\pm}$ annihilation [37,39,40]. While the latter two processes are effective only on small scales $\nu > 10^{-12}$ Hz and do not appear in the currently observed CMB spectra, the former process is effective on large scales with a frequency region $\nu \simeq (10^{-17} \sim 10^{-10})$ Hz, reducing the amplitude of RGWs by ~20% [38]. This in turn will have observable effects on the second and third peaks of C_l^{XX}. Thus, we will employ the RGWs spectrum modified by NFS [38] to calculate C_l^{XX}, improving the previous calculation in Ref. [31] that did not consider the effect of NFS.

In Sec. II we review briefly the result of RGWs spectrum $h(\nu, \eta)$ with modifications due to NFS. In Sec. III we will use this $h(\nu, \eta)$ to compute the spectra C_l^{TT}, C_l^{TE}, C_l^{EE}, and C_l^{BB}. The Basko-Polnarev's method will be used [16,17,41,42]. In the process of the time integration, a fitting formula of the damping factor $D(k)$ on small scales will be introduced, which gives a better representation of the visibility function $V(\eta)$ during the photon decoupling. Section IV examines the influences on C_l^{XX} due to NFS, the spectrum index of inflation, and the fraction of baryon, especially, the corresponding shifting of l_0 of C_l^{TE} is investigated. A summary is given in Sec. V. We use the unit in which $c = \hbar = k_B = 1$ in this paper.

II. RGWS MODIFIED BY NFS

The expansion of a spatially flat ($\Omega_\Lambda + \Omega_m + \Omega_r = 1$) universe can be described by the Robertson-Walker metric

$$ds^2 = a^2(\eta)[-d\eta^2 + (\delta_{ij} + h_{ij})dx^i dx^j], \tag{1}$$

where η is the conformal time and the small perturbation h_{ij} is RGWs and is taken to be traceless and transverse (TT gauge)

$$h^i{}_i = 0, \qquad h^{ij}{}_{,j} = 0. \tag{2}$$

The wave equation of RGWs is

$$\partial_\nu(\sqrt{-g}\partial^\nu h_{ij}) = 0. \tag{3}$$

By the Fourier decomposition

$$h_{ij}(\eta, \mathbf{x}) = \sum_\sigma \int \frac{d^3k}{(2\pi)^3} \epsilon_{ij}^\sigma h_k^{(\sigma)}(\eta) e^{i\mathbf{k}\cdot\mathbf{x}} \tag{4}$$

for each mode $\mathbf{k}$ and each polarization $\sigma = (+, \times)$, Eq. (3) can be put into the form

$$\ddot{h}_k + 2\frac{\dot{a}}{a}\dot{h}_k + k^2 h_k = 0, \tag{5}$$

where $\dot{h}_k = dh_k/d\eta$, the polarization index σ has been skipped for simplicity. Equation (5) holds for most of the stages from the inflationary to the current accelerating expansion. The explicit forms of the scale factor $a(\eta)$ are given:

$$a(\eta) = a_e(\eta - \eta_e), \qquad \eta_s \le \eta \le \eta_2 \tag{6}$$

for the radiation-dominant stage,

$$a(\eta) = a_m(\eta - \eta_m)^2, \qquad \eta_2 \le \eta \le \eta_E \tag{7}$$

for the matter-dominant stage, and

$$a(\eta) = l_H|\eta - \eta_a|^{-\gamma}, \qquad \eta_E \le \eta \le \eta_0 \tag{8}$$

for the accelerating stage up to the present time η_0, where $\gamma \simeq 1.044$ for a dark energy $\Omega_\Lambda \simeq 0.75$, and $l_H = \gamma/H_0$ with H_0 being the Hubble constant. The normalization of $a(\eta)$ is such that $|\eta_0 - \eta_a| = 1$, where $\eta_0 \sim 3.11$. The notations in Eqs. (7) and (8) are adopted from that in Refs. [34,38,39]. In our convention, the conformal time η is dimensionless and the scale factor $a(\eta)$ has the dimension of length. The analytic solution of Eq. (5) and the spectrum are obtained for the expanding universe with the consecutive stages: inflationary, reheating, radiation-dominant, matter-dominant, and accelerating, respectively, in Ref. [34].

As also evidenced by the five-year WMAP [5–8], there exists a cosmic neutrino background with the three light species. By the standard scenario of big bang, during the radiation stage, from the temperature $T \simeq 2$ MeV up to the beginning of the matter domination, the neutrinos are decoupled from other components and start to freely stream in space. This neutrino free-streaming gives rise to an anisotropic portion of the stress tensor, which serves a source for RGWs. Consequently, during this period $\eta_{\nu d} < \eta < \eta_2$, Eq. (5) is modified to the following differential-integral equation [35–38]

$$\ddot{h}_k(\eta) + 2\frac{\dot{a}}{a}\dot{h}_k(\eta) + k^2 h_k(\eta) = -24 f_\nu \left(\frac{\dot{a}}{a}\right)^2 \int_{\eta_{\nu d}}^{\eta} \dot{h}_k(\eta') K(k(\eta - \eta'))d\eta', \tag{9}$$

where the kernel of the integral is

$$K(x) \equiv -\frac{\sin x}{x^3} - \frac{3\cos x}{x^4} + \frac{3\sin x}{x^5} \tag{10}$$

and $f_\nu = \rho_\nu/\rho_0$ is the fractional energy density of neutrinos, whose initial value is $f_\nu(\eta = 0) = 0.405\,23$ for the effective number of species of neutrinos $N_\nu = 3$. The term on the right-hand side of Eq. (9) represents the anisotropic stress tensor due to NFS. $\eta_{\nu d}$ represents the conformal time of neutrino decoupling.

Equation (9) has been solved by perturbations, yielding the full analytic solution $h_k(\eta)$, from the inflation up to the present accelerating stage [38], and it has been found that NFS causes a damping of h_k by ~20% in the frequency range

$$\nu \simeq (10^{-17}, 10^{-10})\ \text{Hz}. \tag{11}$$

Since ν is related to the conformal wave number k as $\nu = \frac{H_0}{2\pi\gamma}k$ with $H_0 = 3.24 \times 10^{-18}h$ Hz being the Hubble frequency, Eq. (11) corresponds to a range of the conformal wave number

$$k \simeq (3 \times 10^1, 3 \times 10^8) \tag{12}$$

for a Hubble parameter $h \simeq 0.7$. NFS also slightly drags the RGWs spectrum to small scales. This dragging effect can be understood by a qualitative analysis. $K(x)$ in Eq. (10) has a peak around $x \sim 0$ and $K(0) \sim 0.07$, and its derivative can be roughly approximated as $K'(x) \simeq -\delta(x)$. The integration on the right-hand side of Eq. (9) can be integrated by parts

$$\int_{\eta_{vd}}^{\eta} \dot{h}_k(\eta')K(\eta - \eta')d\eta' \simeq h_k(\eta)(K(0) - 1). \tag{13}$$

Then Eq. (9) is approximately reduced to

$$\ddot{h}_k + 2\frac{\dot{a}}{a}\dot{h}_k + \left[k^2 - 24f_\nu(1 - K(0))\left(\frac{\dot{a}}{a}\right)^2\right]h_k = 0. \tag{14}$$

By comparing Eq. (14) with Eq. (5), one sees that NFS modifies the squared wave number k^2 to an effective one

$$\bar{k}^2 \equiv k^2 - 24f_\nu(1 - K(0))\left(\frac{\dot{a}}{a}\right)^2 < k^2. \tag{15}$$

If the mode $h_k(\eta)$ without NFS has a peak at $k = k_p$, then the corresponding mode $h_k(\eta)$ with NFS will have a peak at $\bar{k}(k) = k_p$, which yields $k \sim [1 + 12f_\nu(1 - K(0)) \times (\frac{\dot{a}}{a})^2]k_p$. The larger the k_p is, the greater the shifting amount is. This analysis qualitatively explains why NFS slightly drags the peaks of RWGs to large k. It is expected that NFS will cause a slight shift of C_l^{XX} to large l via RGWs consequently.

Since the damping range of RGWs is $(10^{-17}, 10^{-10})$ Hz, its lower frequency part just falls into the observable domain of C_l^{XX}. Therefore, in calculation of CMB spectra, the RGWs damped by NFS should be used as the source. As will be seen in the next section, the mode functions $h_k(\eta_d)$ and $\dot{h}_k(\eta_d)$ at the photon decoupling time η_d, i.e., $z \sim 1100$, will appear in the integral expressions of the spectra of CMB anisotropies and polarizations. They are plotted in Fig. 1. The modifications on $h_k(\eta_d)$ and $\dot{h}_k(\eta_d)$ by NFS leave observable imprints in the spectra of CMB.

As the initial condition, the spectrum of RGWs at the time η_i of the horizon crossing during the inflation is chosen to be [34,38]

$$h(\nu, \eta_i) = \frac{2k^{3/2}}{\pi}|h_k(\eta_i)| = A\left(\frac{k}{k_H}\right)^{2+\beta_{\text{inf}}}, \tag{16}$$

where $k_H = 2\pi$ is the comoving wave number and corresponds to a physical wave $\lambda_H = 2\pi a(\eta_0)/k_H = l_H$, the constant A is to be fixed by the observed CMB anisotropies, and the spectrum index β_{inf} is a parameter determined by inflationary models. The special case of $\beta_{\text{inf}} = -2$ is the de Sitter expansion of inflation. If the inflationary expansion is driven by a scalar field, then the index β_{inf} is related to the so-called slow-roll parameters, η and ϵ [43], as $\beta_{\text{inf}} = -2 + (\eta - 3\epsilon)$. For demonstration purpose in our context, we allow the parameter β_{inf} to take

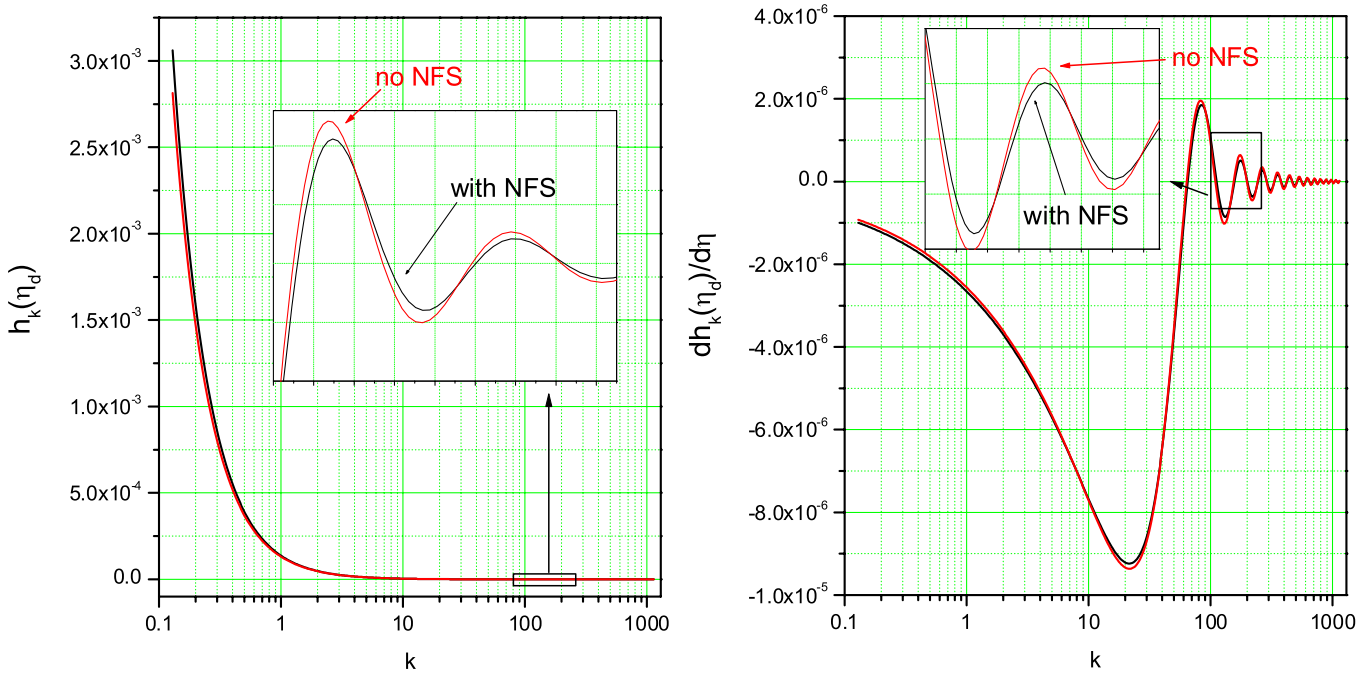

FIG. 1 (color online). The RGWs $h_k(\eta_d)$ and $\dot{h}_k(\eta_d)$ at the decoupling. NFS reduces the amplitudes and shifts the peaks to larger k.

the values > -2. In literature, the RGWs spectrum is often written in terms of $\Delta_h^2(k)$, related to Eq. (16) by $h^2(\nu, \eta_i) = 8\Delta_h^2(k)$. Without the running index, it is usually assumed to have the form [1,2,44]

$$\Delta_h^2(k) = A_T\left(\frac{k}{k_0}\right)^{n_T}. \tag{17}$$

Here the tensorial spectrum index $n_T = 2\beta_{\rm inf} + 4$, k_0 is some comoving pivot wave number, whose corresponding physical wave number is $k_0/a(\eta_H) = 0.002\ {\rm Mpc}^{-1}$ [4,44], and the amplitude $A_T = 2.95 \times 10^{-9} r A(k_0)$ with $A(k_0) \sim 0.8$ as determined by the WMAP observations accordingly [2], r being the tensor/scalar ratio. In general, r is model dependent and frequency dependent [31,32]. The value of r has long been an important issue [45–49]. In our treatment, for simplicity, r is only taken as a constant parameter for normalization of RGWs. Currently, only observational constraints on r have been given. The 1-year WMAP gives $r < 0.71$ [1]. The 3-year WMAP constraint based on the CMB polarization gives $r < 2.2$ (95% C.L.) evaluated at k_0 [4], and the full WMAP constraint is $r < 0.55$ (95% C.L.) [3,4]. Recently, the 5-year WMAP data improves the upper limit to $r < 0.43$ (95% C.L.) [5], and combined with baryon acoustic oscillation and SN gives $r < 0.2$ (95% C.L.) [6,7]. The combination from such observations, as of the Lyman-α forest power spectrum from SDSS, 3-year WMAP, supernovae SN, and galaxy clustering, gives an upper limit $r < 0.22$ (95% C.L.) and $r < 0.37$ (99.9% C.L.) [50]. For concreteness, we take $r \simeq 0.37$ in our calculation.

III. ANALYTICAL SPECTRA OF CMB

In the Basko-Polnarev's method [16,17], the Boltzmann equation of the CMB photon gas for the k mode is written as a set of two coupled differential equations

$$\dot{\xi}_k + [ik\mu + q]\xi_k = \dot{h}_k, \tag{18}$$

$$\dot{\beta}_k + [ik\mu + q]\beta_k = qG_k, \tag{19}$$

where β_k represents the linear polarization, $\alpha_k \equiv \xi_k - \beta_k$ represents the anisotropy of radiation intensity, $\mu = \cos\theta$, q is the differential optical depth, and $G_k(\eta) = \frac{3}{16} \times \int_{-1}^{1} d\mu'[(1+\mu'^2)^2\beta_k - \frac{1}{2}(1-\mu'^2)^2\xi_k]$ [31]. Note that the gravitational wave $\dot{h}_k$ in Eq. (18) is the Sachs-Wolfe term [51] and plays the role of source to the temperature anisotropies. In the following, we omit the subscript k for simplicity of notation. The formal solutions of Eqs. (18) and (19) can be written as

$$\xi(\eta, \mu) = \int_0^\eta \dot{h}(\eta')e^{-\kappa(\eta,\eta')}e^{ik\mu(\eta'-\eta)}d\eta', \tag{20}$$

$$\beta(\eta, \mu) = \int_0^\eta G(\eta')q(\eta')e^{-\kappa(\eta,\eta')}e^{ik\mu(\eta'-\eta)}d\eta', \tag{21}$$

where $\kappa(\eta', \eta) \equiv \int_\eta^{\eta'} q d\eta = \kappa(\eta) - \kappa(\eta')$ with $\kappa(\eta) \equiv \kappa(\eta_0, \eta)$ being the optical depth, such that $q(\eta) = -d\kappa(\eta_0, \eta)/d\eta$. To get rid of the angle dependence, ξ and β are usually decomposed in terms of the Legendre components

$$\xi_l(\eta) = \frac{1}{2}\int_{-1}^{1} d\mu \xi(\eta, \mu)P_l(\mu), \tag{22}$$

$$\beta_l(\eta) = \frac{1}{2}\int_{-1}^{1} d\mu \beta(\eta, \mu)P_l(\mu), \tag{23}$$

where P_l is the Legendre function. Using the expansion formula

$$e^{ix\mu} = \sum_{l=0}^{\infty}(2l+1)i^l j_l(x)P_l(\mu)$$

and the orthonormal relation for Legendre functions, one obtains

$$\xi_l(\eta_0) = i^l \int_0^{\eta_0} e^{-\kappa(\eta)}\dot{h}(\eta)j_l(k(\eta - \eta_0))d\eta, \tag{24}$$

$$\beta_l(\eta_0) = i^l \int_0^{\eta_0} G(\eta)V(\eta)j_l(k(\eta - \eta_0))d\eta, \tag{25}$$

both being evaluated at the present time η_0, where

$$V(\eta) = q(\eta)e^{-\kappa(\eta)} \tag{26}$$

is the visibility function for the decoupling. As is known, $V(\eta)$ is a narrow function peaked around the decoupling time η_d with a width $\Delta\eta_d$. It phenomenologically describes the details of the decoupling process [26,52,53]. Reference [30] uses a single Gaussian function to fit V approximately. In Ref. [31], as an improvement, the following two pieces of the half Gaussian function are used

$$V(\eta) = \begin{cases} V(\eta_d)\exp\left(-\frac{(\eta-\eta_d)^2}{2\Delta\eta_{d1}^2}\right), & (\eta \le \eta_d), \\ V(\eta_d)\exp\left(-\frac{(\eta-\eta_d)^2}{2\Delta\eta_{d2}^2}\right), & (\eta > \eta_d), \end{cases} \tag{27}$$

where the decoupling time $\eta_d \simeq 0.0707$ corresponding to the redshift $z_d \simeq 1100$, $\Delta\eta_{d1} = 0.00639$, $\Delta\eta_{d2} = 0.0117$, and $(\Delta\eta_{d1} + \Delta\eta_{d2})/2 = \Delta\eta_d$ is the thickness of the decoupling. In the absence of reionization, the coefficient $V(\eta_d)$ in Eq. (27) will be determined by the normalization

$$\int_0^{\eta_0} V(\eta)d\eta = 1. \tag{28}$$

We have checked that the error between Eq. (27) to the numerically fitted formula given in Refs. [26,52] is very small, $\sim 3.9\%$ in the interval $\eta > \eta_d$. Compared with the single Gaussian function in Ref. [30], Eq. (27) improves the description of the visibility function by $\sim 10\%$ in accuracy. Substituting Eq. (27) into Eq. (25), after some treatment of the integration over the variable η [31], the

approximate analytic solution of β_l without reionization has been arrived up to the second order of a small $1/q^2$ in the tight coupling limit,

$$\beta_l(\eta_0) = \tfrac{1}{17}\ln\tfrac{20}{3} i^l \Delta\eta_d D(k)\dot{h}(\eta_d) j_l(k(\eta_d - \eta_0)), \quad (29)$$

where $\dot{h}(\eta_d)$ is the time derivative of RGWs at the decoupling, and

$$D(k) = \tfrac{1}{2}[e^{-c(k\Delta\eta_{d1})^2} + e^{-c(k\Delta\eta_{d2})^2}] \quad (30)$$

is the Fourier transformation of $V(\eta)$ in Eqs. (27) with the parameter c taking values in [0, 2]. Formally, the occurrence of the damping factor $D(k)$ is due to the η integration of Eq. (25) of the form $\int_{-\infty}^{\infty} e^{-\eta^2} e^{ip\eta} d\eta = e^{-(p^2/4)} \int_{-\infty}^{\infty} e^{-\eta^2} d\eta$ since the integrand factor $\dot{h}(\eta) j_l(k(\eta - \eta_0))$ contains a mixture of $e^{ik\eta}$ and $e^{-ik\eta}$. From the viewpoint of physics, $D(k)$ is generically expected [26,54], because the photons diffuse through the baryons around the decoupling and the fluctuations are severely damped within the thickness of the surface of the last scattering. Therefore, $D(k)$ is very sensitive to the thickness $\Delta\eta_d$. However, as an approximation, the fitting formula Eq. (30) is not accurate enough on the small scales and will cause an overdamping of amplitudes of C_l^{XX} for larger l. This is because, in the afore-mentioned derivation of Eq. (30), other time-dependent factors in $h_k(\eta)$ have been taken as constants during the decoupling. Besides, other processes important on small scales were not taken into account [26,55]. To improve Eq. (30), we adopt the following simple fitting formula:

$$D(k) = \tfrac{1}{2}[e^{-c(k\Delta\eta_{d1})^b} + e^{-c(k\Delta\eta_{d2})^b}], \quad (31)$$

where b is a parameter. It will find that a good fit with $c \simeq 0.6$ and $b \simeq 0.85$, comparing with the numerical results. One may even effectively simplify Eq. (31) by the following:

$$D(k) = e^{-c(k\Delta\eta_d)^b}. \quad (32)$$

We find that Eqs. (31) and (32) yield the almost overlapping spectra C_l^{XX}, and the error between them is only $\leq 1\%$. In comparison with the numeric computations, C_l^{XX} generated by both Eqs. (31) and (32) are much more accurate than those by Eq. (30).

To evaluate the temperature anisotropies spectrum C_l^{TT}, one needs an analytic solution for α_l. The integrand in (24) contains a factor $e^{-\kappa(\eta)}$, which can be treated approximately. Since the visibility function $V(\eta)$ is a narrow function and can be roughly viewed as a Dirac delta function, so by the relation $V(\eta) = d(e^{-\kappa(\eta_0,\eta)})/d\eta$, one can treat the factor $e^{-\kappa(\eta)}$ as the step function

$$e^{-\kappa(\eta)} \simeq \begin{cases} 0 & (\eta < \eta_d), \\ 1 & (\eta_d < \eta < \eta_0). \end{cases} \quad (33)$$

Substituting Eq. (33) into Eq. (24) yields

$$\xi_l(\eta_0) = i^l \int_{\eta_d}^{\eta_0} \dot{h}(\eta) j_l(k(\eta - \eta_0)) d\eta, \quad (34)$$

which can be integrated by parts,

$$\xi_l(\eta_0) = -i^l h(\eta_d) j_l(k(\eta_d - \eta_0)) + i^l \int_{\eta_d}^{\eta_0} d\eta h(\eta) \frac{d}{d\eta} j_l(k(\eta - \eta_0)), \quad (35)$$

where a term containing $h(\eta_0)$ from the upper limit at η_0 has been neglected since the amplitude $h(\eta_0)$ is about three orders smaller than that of $h(\eta_d)$. The remaining integration term in Eq. (35) is small and can be neglected [41], since $h(\eta)$ is smaller during the late time ($\eta_d \sim \eta_0$) and $\frac{d}{d\eta} j_l$ is the oscillating function. Thus one has the following approximate, analytic solution:

$$\xi_l(\eta_0) = -i^l h(\eta_d) j_l(k(\eta_d - \eta_0)). \quad (36)$$

From Eqs. (29) and (36) follows the temperature anisotropies:

$$\alpha_l(\eta_0) = -i^l j_l(k(\eta_d - \eta_0))[h(\eta_d) + \tfrac{1}{17}\ln\tfrac{20}{3}\Delta\eta_d D(k)\dot{h}(\eta_d)], \quad (37)$$

to which both $h(\eta_d)$ and $\dot{h}(\eta_d)$ contribute. As our calculation shows, the contribution of $\dot{h}(\eta_d)$ is about two orders smaller than that of $h(\eta_d)$.

In terms of α_l and β_l, one calculates C_l^{XX} caused by RGWs [29] straightforwardly. The temperature anisotropies

$$C_l^{TT} = \frac{1}{8\pi}\frac{(l+2)!}{(l-2)!}\int k^2 dk \left| \frac{\alpha_{l-2}(\eta_0)}{(2l-1)(2l+1)} - \frac{2\alpha_l(\eta_0)}{(2l-1)(2l+3)} + \frac{\alpha_{l+2}(\eta_0)}{(2l+1)(2l+3)} \right|^2, \quad (38)$$

the electric type of polarization

$$C_l^{EE} = \frac{1}{16\pi}\int k^2 dk \left| \frac{(l+1)(l+2)\beta_{l-2}(\eta_0)}{(2l-1)(2l+1)} + \frac{6(l-1)(l+2)\beta_l(\eta_0)}{(2l-1)(2l+3)} + \frac{l(l-1)\beta_{l+2}(\eta_0)}{(2l+1)(2l+3)} \right|^2, \quad (39)$$

where the second term in the integrand has the coefficient $6(l-1)(l+2)$, different from that in Ref. [29], the magnetic type of polarization

$$C_l^{BB} = \frac{1}{16\pi}\int k^2 dk \left| \frac{2(l+2)\beta_{l-1}(\eta_0)}{(2l+1)} + \frac{2(l-1)\beta_{l+1}(\eta_0)}{(2l+1)} \right|^2, \quad (40)$$

and the temperature-polarization cross correlation spectrum

$$C_l^{TE} = \sqrt{\frac{1}{8\pi}\frac{(l+2)!}{(l-2)!}}\sqrt{\frac{1}{16\pi}}\int k^2 dk\Big[\frac{\alpha_{l-2}(\eta_0)}{(2l-1)(2l+1)} - \frac{2\alpha_l(\eta_0)}{(2l-1)(2l+3)} + \frac{\alpha_{l+2}(\eta_0)}{(2l+1)(2l+3)}\Big] \times \Big[\frac{(l+1)(l+2)\beta_{l-2}(\eta_0)}{(2l-1)(2l+1)} + \frac{6(l-1)(l+2)\beta_l(\eta_0)}{(2l-1)(2l+3)} + \frac{l(l-1)\beta_{l+2}(\eta_0)}{(2l+1)(2l+3)}\Big], \tag{41}$$

where the second term in the integrand has the coefficient $6(l-1)(l+2)$, different from that in Ref. [29]. Substituting the explicit expressions α_l and β_l of Eqs. (29) and (36) into the above spectra, one finally has

$$C_l^{TT} = \frac{1}{8\pi}\frac{(l+2)!}{(l-2)!}\int k^2 dk P_{Tl}^2(k(\eta_d-\eta_0))\Big|h(\eta_d) + \frac{1}{17}\ln\frac{20}{3}\Delta\eta_d D(k)\dot{h}(\eta_d)\Big|^2, \tag{42}$$

$$C_l^{EE} = \frac{1}{16\pi}\Big(\frac{1}{17}\ln\frac{20}{3}\Big)^2\int k^2 dk P_{El}^2(k(\eta_d-\eta_0)) \times \Delta\eta_d^2 D^2(k)|\dot{h}(\eta_d)|^2, \tag{43}$$

$$C_l^{BB} = \frac{1}{16\pi}\Big(\frac{1}{17}\ln\frac{20}{3}\Big)^2\int k^2 dk P_{Bl}^2(k(\eta_d-\eta_0)) \times \Delta\eta_d^2 D^2(k)|\dot{h}(\eta_d)|^2, \tag{44}$$

$$C_l^{TE} = \frac{1}{136\sqrt{2}\pi}\ln\frac{20}{3}\sqrt{\frac{(l+2)!}{(l-2)!}}\int k^2 dk P_{Tl}(k(\eta_d-\eta_0)) \times P_{El}(k(\eta_d-\eta_0))\frac{1}{2}\Big\{\Big[-h(\eta_d) - \frac{1}{17}\ln\frac{20}{3} \times \Delta\eta_d D(k)\dot{h}(\eta_d)\Big]\dot{h}^*(\eta_d) + \Big[-h^*(\eta_d) - \frac{1}{17}\ln\frac{20}{3} \times \Delta\eta_d D(k)\dot{h}^*(\eta_d)\Big]\dot{h}(\eta_d)\Big\}\Delta\eta_d D(k), \tag{45}$$

where the projection factors are defined as [42]

$$P_{Tl}(x) = \frac{j_{l-2}(x)}{(2l-1)(2l+1)} + \frac{2j_l(x)}{(2l-1)(2l+3)} + \frac{j_{l+2}(x)}{(2l+1)(2l+3)} = \frac{j_l(x)}{x^2}, \tag{46}$$

$$P_{El}(x) = \frac{(l+1)(l+2)}{(2l-1)(2l+1)}j_{l-2}(x) - \frac{6(l-1)(l+2)}{(2l-1)(2l+3)}j_l(x) + \frac{l(l-1)}{(2l+1)(2l+3)}j_{l+2}(x) = -\Big[2 - \frac{l(l-1)}{x^2}\Big]j_l(x) + \frac{2}{x}j_{l-1}(x), \tag{47}$$

$$P_{Bl}(x) = \frac{2(l+2)}{(2l+1)}j_{l-1}(x) - \frac{2(l-1)}{(2l+1)}j_{l+1}(x) = 2j_{l-1}(x) - 2\frac{l-1}{x}j_l(x). \tag{48}$$

With $h(\eta_d)$ and $\dot{h}(\eta_d)$ given from the last section and $D(k)$ from Eq. (31), we compute C_l^{XX} and plot them in Fig. 2, where the following values of respective parameters are taken: the inflationary index $\beta_{\rm inf} = -2.02$, the dark energy $\Omega_\Lambda = 0.75$, the baryon density $\Omega_b = 0.045$, the neutrino species $N_\nu = 3$, and the tensor/scalar ratio $r = 0.37$, $c = 0.6$, and $b = 0.85$. For comparison, in Fig. 2 the numerical results from CAMB [25] are also plotted. It is seen that the analytic C_l^{EE} and C_l^{BB} agree very well with the numerical ones for the range $l \leq 600$ covering the first three peaks, and the error is only $\sim$2%. Comparing with the previous analytic evaluation in Refs. [30,31], our result not only extends the range of validity from $l \leq 300$ to $l \leq 600$, but also improves accuracy substantially.

For the spectra C_l^{TT} and C_l^{TE}, the profiles of our analytic result also agree with the numerical ones fairly well, except that C_l^{TT} is in a range $l \leq 10$ and the first trough of C_l^{TE} around $l \sim 75$ have some deviations. For the purpose of extracting RGWs, more important is C_l^{TE}, whose amplitude at the first trough has a maximum deviation $\sim$20% from that of the numerical CAMB. This is due to the approximation of the temperature anisotropies $\xi_l(\eta_0)$ in Eq. (36), which is not accurate enough for very large scales.

The profiles of C_l^{XX} are largely determined by those of $h(\eta_d)$ and $\dot{h}(\eta_d)$, especially the peaks and troughs of C_l^{XX} correspond to those of RGWs. The integrands for C_l^{XX} in Eqs. (42)–(45) contain the respective projection factors, P_{Tl}, P_{El}, P_{Bl}, which are made of the spherical Bessel's functions. Since $j_l(x)$ is rather sharply peaked around $x \simeq l$ for large l, consequently, the projection factors as functions of k are peaked around

$$k(\eta_0 - \eta_d) \simeq k\eta_0 \simeq l. \tag{49}$$

Therefore, C_l^{XX} as integrations over k will receive major contributions from the integration domain $k \sim l/\eta_0$ [31]:

$$C_l^{TT} \propto |h(\eta_d)|^2_{k\simeq l/\eta_0}, \tag{50}$$

$$C_l^{EE}, C_l^{BB} \propto |\dot{h}(\eta_d)|^2_{k\simeq l/\eta_0} D^2(k), \tag{51}$$

$$C_l^{TE} \propto h(\eta_d)\dot{h}(\eta_d)_{k\simeq l/\eta_0} D(k). \tag{52}$$

By Eq. (50), the locations of the peaks of C_l^{TT} is mainly determined by $|h(\eta_d)|^2$. Indeed, the right panel in Fig. 3 shows that the peaks and troughs of C_l^{TT} correspond to those of $|h(\eta_d)|^2$. Similarly, by Eq. (51), the locations of the peaks of C_l^{EE} and C_l^{BB} correspond to those of $|\dot{h}(\eta_d)|^2$, shown in the left panel in Fig. 3. The similar correspondence, as revealed by Eq. (52), of the locations of the peaks of C_l^{TE} to those of $h(\eta_d)\dot{h}(\eta_d)_k$ is also confirmed, but the

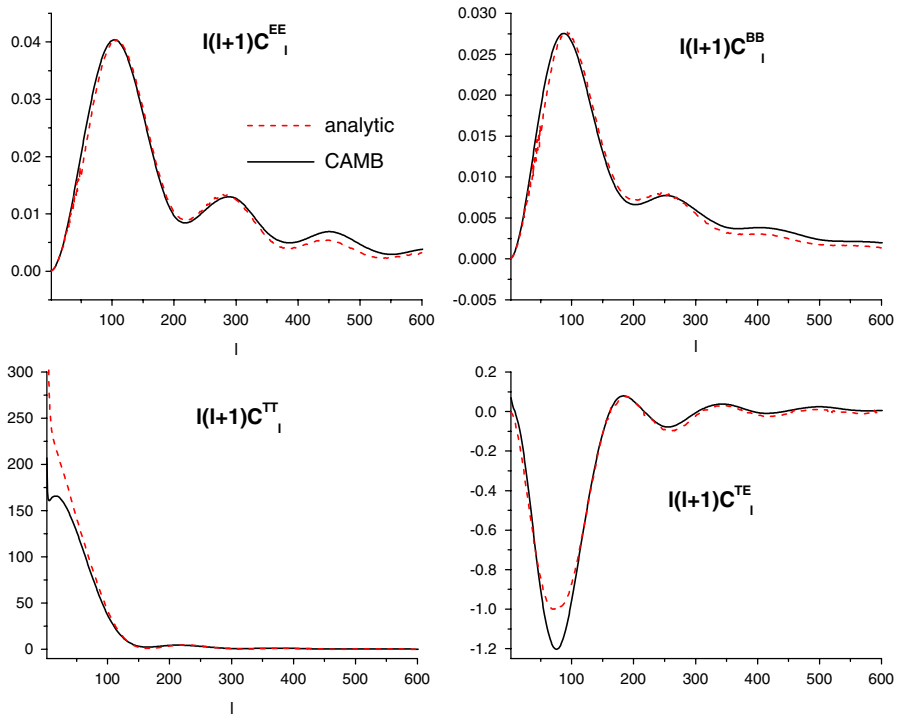

FIG. 2 (color online). The analytic spectra C_l^{XX} generated by RGWs are compared with the numeric ones from CAMB [25]. Here the decay factor $D(k)$ in Eq. (31) has been used.

graph is not presented though in order to save room. Besides, C_l^{EE}, C_l^{BB}, and C_l^{TE} also depend on the damping factor $D(k)$, leading to the strong damping of C_l^{EE}, C_l^{BB}, and C_l^{TE} at large l, as shown in Fig. 2 and 3. Overall, our analytic formulation yields a good approximation of C_l^{XX} in comparison with the numerical results.

We use the data from 5-year WMAP [7,8] to limit the B-mode polarization C_l^{BB} generated by RGWs in Fig. 4. It is seen that the current observational data can only put a rather loose limit on RGWs. For $r = 0.37$ the amplitude of the predicted spectrum is about 2 orders below the upper limit by WMAP5. Improvements on the limit, or possible direct detections of C_l^{BB} are expected from more sensitive polarization measurements by upcoming experiments, such as Clover [56], EBEX [57], Spider [58], and Planck [59].

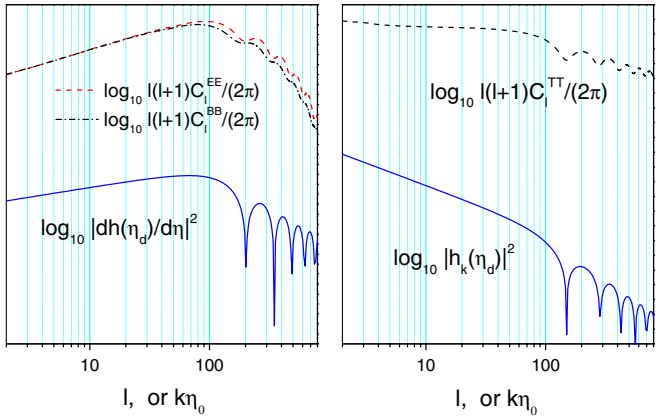

FIG. 3 (color online). The left panel: the locations of peaks C_l^{EE} and C_l^{BB} correspond to that of $|\dot{h}_k(\eta_d)|^2$. The right panel: the locations of peaks of C_l^{TT} correspond to that of $|h_k(\eta_d)|^2$. Here $|\dot{h}_k(\eta_d)|^2$ and $|h_k(\eta_d)|^2$ have been plotted with the variable $k\eta_0$, which is $\sim l$ by Eq. (49).

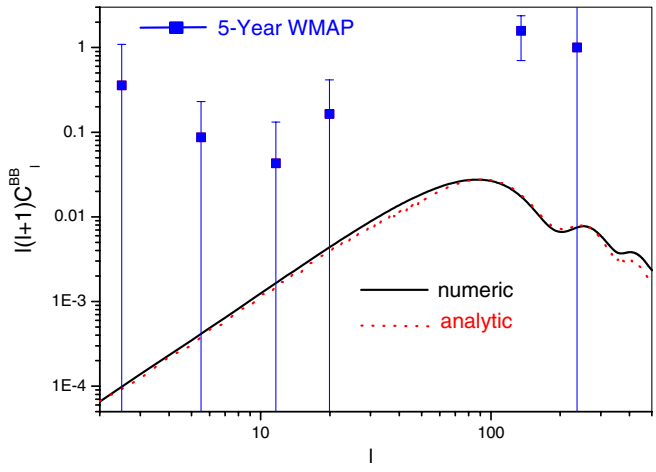

FIG. 4 (color online). The predicted C_l^{BB} is well below the constraint of the 5-year WMAP data [7,8]. Here the tensor/scalar ratio $r = 0.37$ is taken in computation.

IV. INFLUENCES BY NFS, INFLATION, AND BARYONS

A. The NFS

Let us analyze the effect of NFS on the spectra C_l^{XX}. To demonstrate this, the spectra C_l^{XX} with and without NFS are plotted in Fig. 5. The $l \leq 100$ portion of the spectra are not affected much by NFS, only on the scales of $l > 200$ are the spectra modified effectively. The reduction of amplitudes of C_l^{TT}, C_l^{EE}, and C_l^{BB} by NFS is noticeable only starting from the second peak. For instance, the third peak of C_l^{TT} is reduced by $\sim$25% and the fourth peak by $\sim$35%. Similar modifications also occur in the spectra C_l^{EE}, C_l^{BB}, and C_l^{TE}. These features of modifications can be understood as follows. As shown in Eq. (12), the damping of RGWs is effective for the conformal wave numbers $k > 30$, which, by the relation in Eq. (49), means that only those portions with $l \geq 100$ of CMB spectra will be affected by NFS. Besides, Fig. 5 also shows that NFS causes a slight shift of the peak locations of C_l^{XX} to larger l, a feature to be expected, since NFS shifts the peaks of $h(\eta_d)$ and $\dot{h}(\eta_d)$ slightly to large k, the peaks of C_l^{XX} will be accordingly shifted to larger l by Eqs. (49)–(52). Given the current precision level of observations on CMB, these small modifications caused by NFS will be difficult to detect at the moment.

As mentioned in the introduction, the cross spectrum C_l^{TE} can be useful in revealing the presence of RGWs in the zero-multipole method [32,33,41,42,60]. The 5-year WMAP [7,8] has given the observed C_l^{TE}, which is negative (anticorrelation) in a range $l \simeq (50, 220)$. Theoretically, it is a combination of contributions of the density perturbations and the RGWs as well. To search for the evidence of RGWs, one needs to disentangle the contribution of RGWs from the total. The inclusion of NFS into the calculation will cause a shifting of the position of the peaks of C_l^{TE} to larger values of l, and Δl tends to increase with l. For instance, Fig. 5 shows that, without NFS, $C_l^{TE} < 0$ for $l \leq 136$ and $C_l^{TE} > 0$ for $l \simeq (137, 179)$. When NFS is included, $C_l^{TE} < 0$ for $l \leq 136$, $C_l^{TE} > 0$ for $l \simeq (137, 183)$. In this low l region the shifting due to NFS is small $\Delta l \leq 4$. But, in the large l region the shifting is large, say, around $l \simeq 500$, it is $\Delta l \sim 10$. This analysis tells us that the zero multipole around $l_0 \sim 50$ is not strongly affected by NFS. However, if we look at the second zero multipole $l \sim 220$, at which C_l^{TE} crosses 0 once again and turns positive, the influence by NFS is rather strong, $\Delta l \sim 5$. More accurate observations of C_l^{TE} and a detailed analysis are needed before a definite conclusion can be drawn on the existence of RGWs.

B. The inflation

The CMB spectra generated by RGWs depend very sensitively on the initial spectrum $h(\nu, \eta_i)$ during the inflationary stage. For the power-law form of $h(\nu, \eta_i)$ in Eq. (16), C_l^{XX} depend on both the amplitude A and the index $\beta_{\rm inf}$. Figure 6 shows C_l^{XX} for the cases of $\beta_{\rm inf} = -1.8$ and -2.02 with NFS being taken into account. A larger index $\beta_{\rm inf}$ yields higher amplitudes of C_l^{EE} and C_l^{BB} in the whole

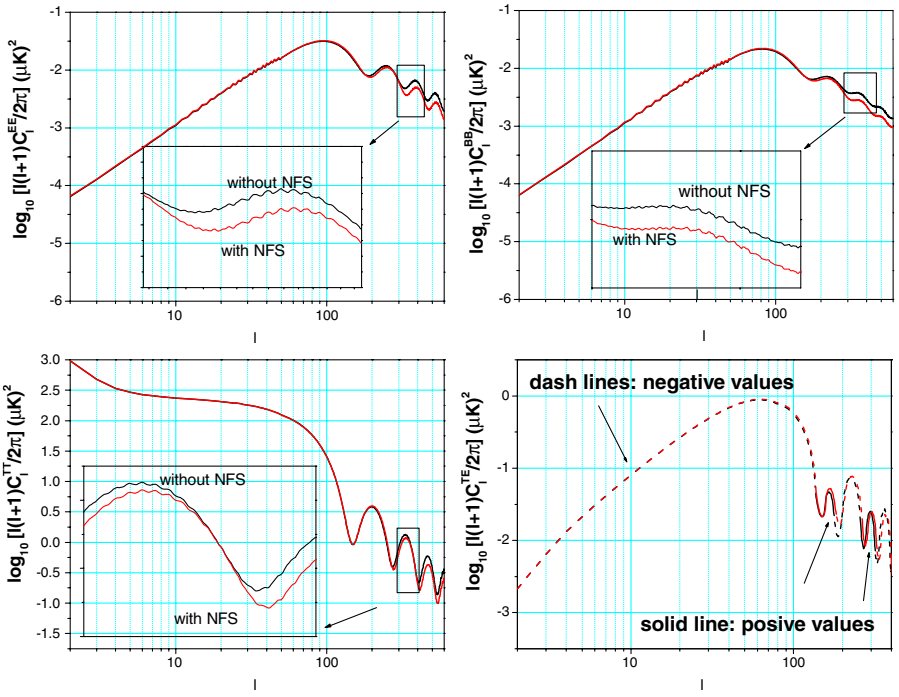

FIG. 5 (color online). The NFS modifications on C_l^{XX} are demonstrated. For $l \leq 600$, the amplitudes are reduced by up to $\sim$35% and the peaks are shifted to larger l by NFS.

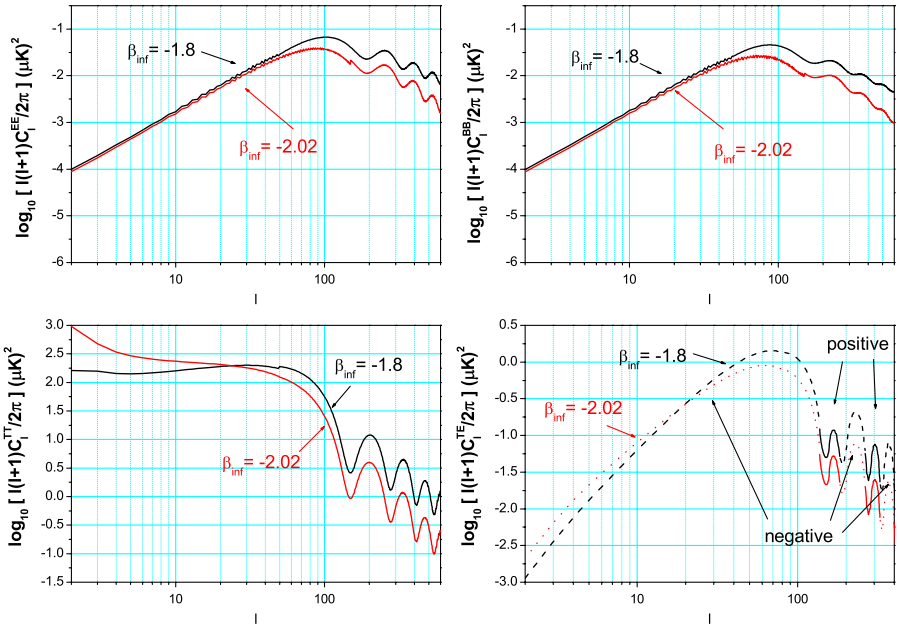

FIG. 6 (color online). C_l^{XX} are sensitive to the inflation index $\beta_{\rm inf}$ of RGWs. Two cases are plotted for $\beta_{\rm inf} = -1.8$ and -2.02. A larger $\beta_{\rm inf}$ yields higher amplitudes of C_l^{EE} and C_l^{BB}.

range of l, agreeing with the previous result [34], and higher amplitude of C_l^{TT} for the range $l > 20$. In the zero-multipole method, one is more interested in C_l^{TE} in the narrow range $l \simeq (40, 60)$, in which the first zero multipole l_0 should appear. First, as Fig. 6 shows, C_l^{TE} is negative in this range, and moreover, a larger index $\beta_{\rm inf}(= -1.8)$ yields a steeper, down slope of C_l^{TE} of negative amplitude. With other parameters being fixed, a larger index $\beta_{\rm inf}$ tends to shift the value of the zero multipole l_0 of C_l^{TE} to larger l. For instance, our calculation shows that, relative to the WMAP-preferred $\beta_{\rm inf} = -2.02$ case, the exact de Sitter $\beta_{\rm inf} = -2$ case shifts l_0 to a larger value by $\Delta l \sim 1$, and the less-preferred case $\beta_{\rm inf} = -1.8$ shifts l_0 by $\Delta l \sim 8$.

Notice that, for C_l^{TT} around $l \sim 20$, the two curves for $\beta_{\rm inf} = -1.8$ and for $\beta_{\rm inf} = -2.02$ intercept. A similar

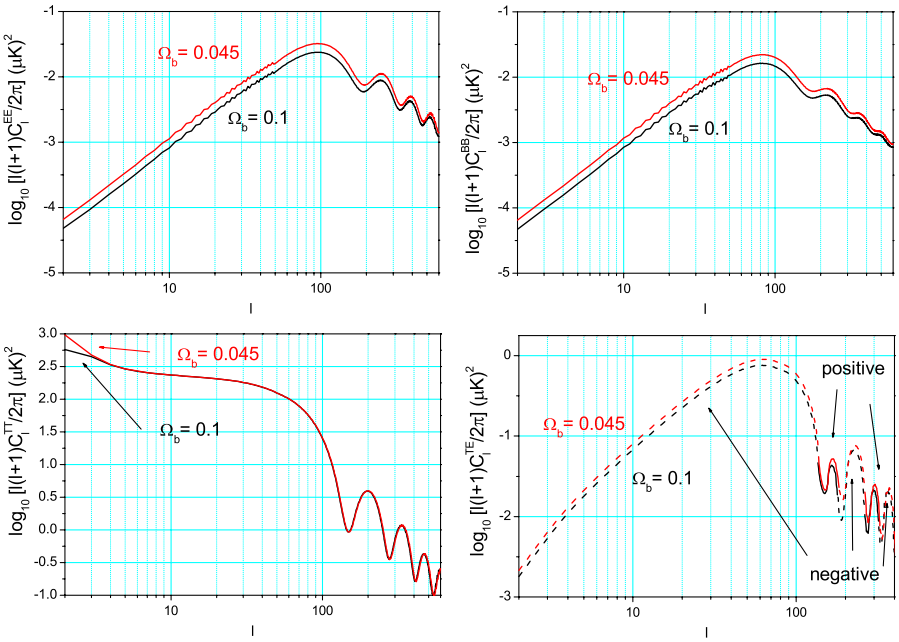

FIG. 7 (color online). The baryon fraction Ω_b affects C_l^{XX}. Two cases are given for $\Omega_b = 0.1$ and 0.045. A larger Ω_b yields lower amplitudes of C_l^{EE}, C_l^{BB}, and C_l^{TE}.

interception also occurs for C_l^{TE} as well. This behavior can be understood as the following. The initial spectrum of RGWs in Eq. (16) contains a factor $(\frac{k}{k_0})^{2+\beta_{\rm inf}}$ with the comoving pivot wave number $k_0 \simeq 6h^{-1}$. On large scales $k < k_0$, one has $(\frac{k}{k_0})^{2+\beta_{\rm inf}} < 1$ for $\beta_{\rm inf} = -1.8$, and $(\frac{k}{k_0})^{2+\beta_{\rm inf}} > 1$ for $\beta_{\rm inf} = -2.02$. By the relation in Eq. (49), the corresponding pivot multipole is $l \simeq k\eta_0 \simeq 20$. Thus, in the region of $l < 20$, C_l^{TT} and C_l^{TE} have lower amplitude for $\beta_{\rm inf} = -1.8$ and higher amplitude for $\beta_{\rm inf} = -2.02$.

C. The baryon density Ω_b

The wave equation (5) of RGWs is not explicitly coupled with the baryons. As a result, $h_k(\eta)$ and $\dot{h}_k(\eta)$ are not very sensitive to the baryons. The impact on CMB by the baryons are mainly through the Thompson scattering terms, $q\xi_k$, $q\beta_k$, and qG_k, in Boltzmann's equation of photons (18) and (19). During the evolution of CMB, the photon decoupling process is particularly important, which depends sensitively on the baryon component. The fitting formula of the visibility function $V(\eta)$ given in Ref. [26] contains explicitly the baryon fraction Ω_b. A larger Ω_b yields a larger decoupling time η_d and a smaller decoupling width $\Delta\eta_d$ [31]. Moreover, in Eqs. (42) through (45), the integrands contain $h(\eta_d)$, $\dot{h}(\eta_d)$, and $\Delta\eta_d D(k)$, which are functions of η_d and $\Delta\eta_d$. We plot C_l^{XX} for $\Omega_b = 0.045$ and 0.1 in Fig. 7. It is seen that the amplitudes of C_l^{EE} and C_l^{BB} with $\Omega_b = 0.045$ are slightly higher than those of $\Omega_b = 0.1$. Thus, a larger Ω_b gives a lower amplitude of C_l^{EE} and C_l^{BB}, agreeing with the previous calculations [31]. As a new result of this paper, Fig. 7 also shows that a smaller Ω_b yields a higher amplitude of C_l^{TE} and shifts the value of the zero multipole l_0 to large l. For instance, $\Omega_b = 0.045$ shifts l_0 to a large value by $\Delta l \sim 2$ relative to the $\Omega_b = 0.1$ case. Besides, C_l^{TT} is less sensitive to the value of Ω_b than the other three spectra.

V. SUMMARY

In this paper we have presented the approximate, analytical formulae of the four CMB spectra generated by RGWs. This has been motivated by an attempt to extract signals of RGWs possibly already contained in C_l^{XX}, especially in the magnetic polarization spectrum C_l^{BB} and the cross spectrum C_l^{TE}.

In our calculation, a fitting formula of the exponentially damping factor $D(k)$, in Eqs. (31) or (32), has been introduced to describe the decoupling process effectively. The resulting analytic spectra C_l^{EE} and C_l^{BB} agree quite well with the numerical ones from CAMB on large scales for the first three peaks for $l \leq 600$, and the error is only $\sim 3\%$. This improves substantially both the precision and the range of validity in comparison with the previous analytic studies. The spectra C_l^{TT} and C_l^{TE} are first analytically computed in this paper. They have overall profiles agreeing with the numerical ones, but their amplitudes have certain deviations due to the approximation adopted in Eq. (36). More relevant to us is C_l^{TE}, whose amplitude of the 1st trough at $l \sim 75$ has a maximum deviation $\sim 20\%$. An analytic formulation of $\xi(\eta_0)$ better than Eq. (36) should be aimed at in future work.

For the Sachs-Wolfe term in the Boltzmann's equation for photons, we have included the damping effect of NFS on the RGWs $h_k(\eta)$ as the source. As is expected, NFS appreciably reduces the amplitudes of C_l^{XX} for large $l > 100$ and, at the same time, shifts slightly the locations of the peaks to large l. Thus, in the zero multiple method by examining the positions where C_l^{TE} crosses 0, the shifting due to the NFS effect should be taken into account for a complete analysis.

We have also demonstrated the influences on C_l^{XX} by the tensorial spectrum index $\beta_{\rm inf}$ of the inflation and the baryon fraction Ω_b. It is found that a larger $\beta_{\rm inf}$ leads to a higher amplitude of CMB spectra, whereas the larger Ω_b gives a lower one. Both of them shift the locations of the peaks of C_l^{XX}. In regard to the shifting of the zero multipoles l_0 of C_l^{TE}, NFS is as important as the inflation and the baryons and should be included in any comprehensive study.

ACKNOWLEDGMENTS

T. Y. Xia's work is partially supported by Graduate Student Research Funding from USTC. Y. Zhang's research work is supported by the CNSF No. 10773009, SRFDP, and CAS. We thank Dr. W. Zhao and Z. Cai for interesting discussions.

[1] D. N. Spergel *et al.*, Astrophys. J. Suppl. Ser. **148**, 175 (2003).
[2] H. V. Peiris *et al.*, Astrophys. J. Suppl. Ser. **148**, 213 (2003).
[3] D. N. Spergel *et al.*, Astrophys. J. Suppl. Ser. **170**, 377 (2007).
[4] L. Page *et al.*, Astrophys. J. Suppl. Ser. **170**, 335 (2007).
[5] J. Dunkley *et al.*, arXiv:0803.0586.
[6] G. Hinshaw *et al.*, arViv:0803.0732.
[7] E. Komatsu *et al.*, arXiv:0803.0547.
[8] M. R. Nolta *et al.*, arViv:0803.0593.
[9] S. Sasaki, Prog. Theor. Phys. **76**, 1036 (1986).
[10] W. Hu and S. Dodelson, Annu. Rev. Astron. Astrophys. **40**, 171 (2002).

[11] V. A. Rubakov, M. Sazhin, and A. Veryaskin, Phys. Lett. B **115**, 189 (1982).
[12] R. Fabbri and M. D. Pollock, Phys. Lett. B **125**, 445 (1983).
[13] L. Abbott and M. Wise, Nucl. Phys. **B237**, 226 (1984).
[14] A. Starobinskii, Sov. Astron. Lett. **11**, 133 (1985).
[15] V. F. Mukhanov, H. A. Feldman, and R. H. Brandenberger, Phys. Rep. **215**, 203 (1992).
[16] M. M. Basko and A. G. Polnarev, Mon. Not. R. Astron. Soc. **191**, 207 (1980).
[17] A. Polnarev, Sov. Astron. **29**, 607 (1985).
[18] W. Zhao and Y. Zhang, Phys. Rev. D **74**, 043503 (2006).
[19] B. Abbott *et al.*, Phys. Rev. D **77**, 022001 (2008).
[20] A. M. Cruise and R. M. J. Ingley, Classical Quantum Gravity **22**, s479 (2005); **23**, 6185 (2006).
[21] M. L. Tong and Y. Zhang, Chin. J. Astron. Astrophys. **8**, 314 (2008).
[22] F. Y. Li, M. X. Tang, J. Luo, and Y. C. Li, Phys. Rev. D **62**, 044018 (2000).
[23] M. L. Tong, Y. Zhang, and F. Y. Li, Phys. Rev. D **78**, 024041 (2008).
[24] U. Seljak and M. Zaldarriaga, Astrophys. J. **469**, 437 (1996); http://lambda.gsfc.nasa.gov/toolbox/tb_cmbfast_-form.cfm.
[25] A. Lewis, A. Challinor, and A. Lasenby, Astrophys. J. **538**, 473 (2000); http://lambda.gsfc.nasa.gov/toolbox/tb_camb_form.cfm.
[26] W. Hu and N. Sugiyama, Astrophys. J. **444**, 489 (1995).
[27] M. Zaldarriaga and D. D. Harari, Phys. Rev. D **52**, 3276 (1995).
[28] L. P. Grishchuk, Phys. Rev. D **48**, 3513 (1993); Phys. Rev. Lett. **70**, 2371 (1993).
[29] M. Kamionkowski, A. Kosowsky, and A. Stebbins, Phys. Rev. D **55**, 7368 (1997).
[30] J. Pritchard and M. Kamionkowski, Ann. Phys. (N.Y.) **318**, 2 (2005).
[31] W. Zhao and Y. Zhang, Phys. Rev. D **74**, 083006 (2006).
[32] D. Baskaran, L. P. Grishchuk, and A. G. Polnarev, Phys. Rev. D **74**, 083008 (2006).
[33] A. G. Polnarev, N. J. Miller, and B. G. Keating, Mon. Not. R. Astron. Soc. **386**, 1053 (2008); N. J. Miller, B. G. Keating, and A. G. Polnarev, arXiv:0710.3651.
[34] Y. Zhang *et al.*, Classical Quantum Gravity **22**, 1383 (2005); **23**, 3783 (2006).
[35] S. Weinberg, Phys. Rev. D **69**, 023503 (2004).
[36] D. A. Dicus and W. W. Repko, Phys. Rev. D **72**, 088302 (2005).
[37] Y. Watanabe and E. Komatsu, Phys. Rev. D **73**, 123515 (2006).
[38] H. X. Miao and Y. Zhang, Phys. Rev. D **75**, 104009 (2007).
[39] S. Wang, Y. Zhang, T. Y. Xia, and H. X. Miao, Phys. Rev. D **77**, 104016 (2008).
[40] D. J. Schwarz, Mod. Phys. Lett. A **13**, 2771 (1998).
[41] D. Baskaran, L. P. Grishchuk, and A. G. Polnarev, Phys. Rev. D **74**, 083008 (2006).
[42] B. Keating, A. Polnarev, N. Miller, and D. Baskaran, Int. J. Mod. Phys. A **21**, 2459 (2006).
[43] A. R. Liddle and D. H. Lyth, Phys. Lett. B **291**, 391 (1992).
[44] L. Verde *et al.*, Astrophys. J. Suppl. Ser. **148**, 195 (2003).
[45] U. Seljak *et al.*, Phys. Rev. D **71**, 103515 (2005).
[46] A. Cooray, P. S. Corasaniti, T. Giannantonio, and A. Melchiorri, Phys. Rev. D **72**, 023514 (2005).
[47] T. L. Smith, M. Kamionkowski, and A. Cooray, Phys. Rev. D **73**, 023504 (2006); Phys. Rev. D **78**, 083525 (2008).
[48] A. Linde, V. Mukhanov, and M. Sasaki, J. Cosmol. Astropart. Phys. 10 (2005) 002.
[49] V. Mukhanov and A. Vikman, J. Cosmol. Astropart. Phys. 02 (2006) 004.
[50] U. Seljak, A. Slosar, and P. McDonald, J. Cosmol. Astropart. Phys. 10 (2006) 014.
[51] R. K. Sachs and Q. M. Wolfe, Astrophys. J. **147**, 73 (1967).
[52] B. J. T. Jones and R. F. G. Wyse, Astron. Astrophys. **149**, 144 (1985).
[53] P. J. E. Peebles, Astrophys. J. **153**, 1 (1968).
[54] P. J. E. Peebles, *The Large Scale Structure of the Universe* (Princeton University Press, Princeton, NJ, 1980).
[55] J. M. Bardeen, J. R Bond, N. Kaiser, and A. S. Szalay, Astrophys. J. **304**, 15 (1986).
[56] A. C. Taylor, New Astron. Rev. **50**, 993 (2006); C. North *et al.*, arXiv:astro-ph/0805.3690.
[57] http://group.physics.umn.edu./cosmology/ebex.html; P. Oxley *et al.*, Proc. SPIE Int. Soc. Opt. Eng. **5543**, 320 (2004).
[58] C. J. MacTavish *et al.*, arXiv:astro-ph/0807.1548.
[59] http://www.rssd.esa.int/index.php?project=Planck.
[60] L. P. Grishchuk, arXic:0707.3319